IEEE TRANSACTIONS ON

NEURAL SYSTEMS AND REHABILITATION ENGINEERING

A PUBLICATION OF THE IEEE ENGINEERING IN MEDICINE AND BIOLOGY SOCIETY

Indexed in the National Library of Medicine, PubMed®, and MEDLINE®

DECEMBER 2007 VOLUME 15 NUMBER 4 ITNSB3 (ISSN 1534-4320)

REGULAR PAPERS

Neural Engineering

Rehabilitation Engineering

(Contents Continued on Back Cover)

(Contents Continued from Front Cover)

Design, Implementation and Clinical Tests of a Wire-Based Robot for Neurorehabilitation

Giulio Rosati, Paolo Gallina, and Stefano Masiero

***Abstract*—This paper presents the development of and clinical tests on NeReBot (NEuroREhabilitation roBOT): a three degrees-of-freedom (DoF), wire-driven robot for poststroke upper-limb rehabilitation. Basically, the robot consists of a set of three wires independently driven by three electric motors. The wires are connected to the patient's upper limb by means of a splint and are supported by a transportable frame, located above the patient. By controlling wire length, rehabilitation treatment (based on the passive or active-assistive spatial motion of the limb) can be delivered over a wide working space. The arm trajectory is set by the therapist through a very simple teaching-by-showing procedure, enabling most common "hands on" therapy exercises to be reproduced by the robot. Compared to other rehabilitation robots, NeReBot offers the advantages of a low-cost mechanical structure, intrinsically safe treatment thanks to the use of wires, high acceptability by the patient, who does not feel constrained by an "industrial-like" robot, transportability (it can be easily placed aside a hospital bed and/or a wheelchair), and a good trade-off between low number of DoF and spatial performance. These features and the very encouraging results of the first clinical trials make the NeReBot a good candidate for adoption in the rehabilitation treatment of subacute stroke survivors. Clinical trials were performed with a 12-patient experimental group and a 12-patient control group. Resulted that the patients who received robotic therapy in addition to conventional therapy showed greater reductions in motor impairment (in terms of Medical Research Council score, the upper limb subsection of the Fugl–Meyer score, and the Motor Status Score) and improvements in functional abilities (as measured by the Functional Independence Measure and its motor component). No adverse effects occurred and the robotic approach was very well accepted. According to these results, the NeReBot therapy may efficaciously complement standard post-stroke multidisciplinary rehabilitation and offer novel therapeutic strategies for neurological rehabilitation.**

***Index Terms*—Rehabilitation, stroke, subacute phase, upper limb, wire-driven robot.**

I. Introduction

THE rehabilitation goal in poststroke hemiplegic subjects is to promote recovery of lost function, leading to independence and early reintegration into social and domestic life, and reduce the degree of permanent disability. Technology can now permit delivery of robot-aided neurological rehabilitation treatment in a safe, reliable, effective manner. However, dedicated machines need to be further fine-tuned to make them work in the real healthcare environment. Great effort is thus required to find the best trade-off between low cost systems and functional outcome benefits. Machines should be easy to transport, especially in the treatment of subacute patients (i.e., at the start of intensive rehabilitation treatment which is usually within the first two weeks poststroke) [1]. Moreover, it must be reliable and easy to use, since in most cases it will be programmed by nontechnical staff (physicians and physiatrists).

The integration of robotic therapy into current practice may increase therapists' efficiency and effectiveness by alleviating labor-intensive aspects of physical rehabilitation [2], [3], i.e., therapy can last longer and several patients can be treated at the same time under the supervision of a single therapist. The use of robotic devices in rehabilitation can provide high-intensity, repetitive, task-specific, interactive treatment of the impaired upper limb and can serve as an objective, reliable means of monitoring patient progress. High-intensity, task-specific upper-limb treatment consisting of passive or active, highly repetitive movements is one of the most effective approaches to arm and hand-function restoration [4], [5]. Robotic devices can be used to manipulate the paretic arm by high intensity, task-specific movements rather like physical therapy exercises, i.e., by repetitive movements guided through a stereotyped pattern. Feys *et al.* [6] have shown that highly repetitive, stereotyped movements can be effective in stroke subjects if the movements are facilitated by external forces applied to the limb. Nonetheless, robot-assisted rehabilitation is not just a matter of increased productivity. There is evidence that the practice of repetitive movements (passive, active assistive, active) can affect recovery from brain injury [7]. As far as upper limb rehabilitation is concerned, several authors have reported encouraging results when the intensity of standard physical therapy treatment is increased [7], [8]. Other studies have shown that the repetitive practice of hand and finger movements against loads resulted in greater improvements in motor performance and function scales than did Bobath-based treatment [8].

The most famous, most successful example of a robot designed for neurorehabilitation is probably the MIT-Manus [9]. It consists of a two-DoF, two-link serial robot that can guide or interact with the patient's arm over a plane workspace. The patient's forearm is fixed to the robot's end-effector by means of a splint. The robot features torque sensors and a virtual interface to provide patients with different training scenarios.

Manuscript received January 23, 2006; revised May 22, 2007; accepted May 23, 2007. This work was supported by the Italian Ministry of University and Research (MIUR).

G. Rosati is with the Department of Innovation in Mechanics and Management (DIMEG), University of Padua, 35131 Padua, Italy.

P. Gallina is with the Department of Energetics, University of Trieste, 34127 Trieste, Italy.

S. Masiero is with the Unit of Rehabilitation, Department of Medical and Surgical Sciences, University of Padua, 35128 Padua, Italy.

Color versions of one or more of the figures in this paper are available online at http://ieeexplore.ieee.org.

Digital Object Identifier 10.1109/TNSRE.2007.908560

Although the effectiveness of the MIT-Manus has been proven by clinical tests, this robot cannot provide all the typical movements required by conventional therapy, especially out-of-plane movements. To overcome this limitation, other approaches have been proposed. A spatial working space is usually obtained by means of multi-DoF serial robots. Some examples are as follows.

- The ARM (Assisted Rehabilitation and Measurement) Guide, a singly-actuated robotic device, which consists of a handpiece attached to an orientable linear track [10]; although such a robot allows spatial movements, its frame results heavyweight and the motion quality is affected by high inertia because of the presence of balancing masses.
- The MIME, a 6-DoF Puma robot arm which is attached to the arm support on the patient's paretic side; the device moves the limb in simple predetermined trajectories by directly controlling the position and orientation of the forearm [11]; like most industrial robots, the Puma robot is meant to operate in an operator-free area, due to its ability to produce high forces at high speed that could be dangerous for patients; for this reason, we believe that industrial robots do not represent a key tool for the future of robot-assisted rehabilitation.
- The ARMin, a wall-mounted 6-DoF exoskeleton [12]; an exoskeleton is capable to perfectly fit around the patient's arm, providing all the required movements; the main disadvantage of such a robot consists in the complexity of setting the patient's arm inside the robot itself; moreover, exoskeletons are usually complicated to realize because of the high number of mechanical components.
- The REHAROB, a robotic system based on two ABB industrial robots [13].

Unfortunately, these and other serial structure robots are heavyweight machines, which are not easily transportable and not intrinsically safe should a fault occur in the hardware or software.

The patient's upper limb can be guided along a spatial path by means of wire-driven robots. Such robots are light and intrinsically safe for patients and therapists thanks to the wire actuation system. On the contrary, serial structure robots are composed of rigid links which, in the event of failure, can hurt people sharing the same working space. This is the main reason why industrial robots are always employed in conjunction with guarding systems such as enclosures and barriers. Conversely, wire-based robots do not have moving rigid links. Moreover, wires are compliant and nearly massless. While redundant safety systems must clearly always be implemented, this kind of machine is less likely to hurt the patient in the event of failure. Finally, patients and/or human operators do not feel constrained by wire-based robots. This is a key aspect to consider during the design process since patients and/or users tend to reject robotic or other high-tech assistance on emotional grounds [14], [15]. The rehabilitation field provides some examples of wire-based robots. For instance, Takahashi and Kobayashi [16] proposed an upper limb motion robot for disabled people. Another example is SPIDAR-G, a 7-DoF wire-based robot implemented at the Tokyo Institute of Technology, which allows users to interact with virtual objects by manipulating two hemispherical grips [17]. More recently, the Gentle/s project proposed an interesting combination of wire-driven technology and serial robotic structures [18]. Another wire robotic system, the STRING-MAN, employs the wire-drive philosophy for gait rehabilitation [19]. Nowadays, only a few of these robotic devices have been tested in a clinical environment (mainly the Gentle/s, whose pilot study on 30 patients gave results in accordance with findings of the MIT-MANUS studies [18]).

Fig. 1. NeReBot overall view. Patient's forearm is fastened onto a splint, which is moved by three directly-driven nylon wires. Graphical interface is used to keep the patient's attention focused on the exercise.

All these wire-based robots are typically cumbersome and cannot be transported inside a clinical environment or employed for domestic rehabilitation, since they require complex, stable structures to support the wires. Moreover, they cannot be used to deliver proper assisted therapy to sub-acute post-stroke patients who need to lie in bed. Taking into account all the aforesaid requirements and drawbacks, a new wire-based robot, named NeReBot (NEuroREhabilitation roBOT), was designed and built at the Department of Innovation in Mechanics and Management, University of Padua, Padua, Italy [20], [21]. The principle is very simple: once the patient's forearm is fastened onto the splint, the machine can produce stimulation of the upper limb by pulling three nylon wires (see Fig. 1). The main features of NeReBot are as follows.

- It is a 3-DoF wire-driven robot, whose end-effector moves inside a spatial working space.
- The patient does not have the unpleasant feeling of being restrained by a machine.
- It is transportable and it can be easily stored after treatment.
- It can deliver therapy while patients are sitting on a chair or lying in bed.
- The robot frame can be manually set to achieve different tasks and different patient positions.

These considerations suggest that NeReBot can be effectively employed in rehabilitation of the upper limb of hemiplegic stroke survivors. This especially applies during the subacute phase (early intensive rehabilitation treatment may produce

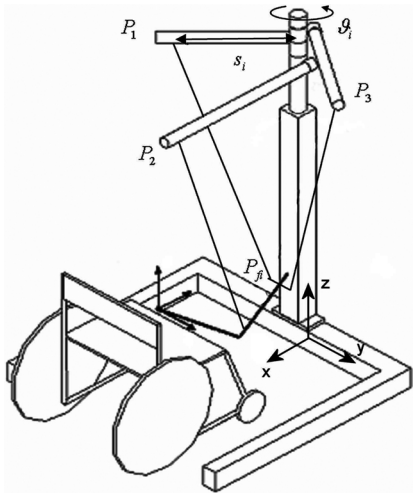

Fig. 2. Diagram of the NeReBot structure. Each horizontal arm can be adjusted by setting its rotation ϑ_i and by choosing the distance s_i of ith wire entry point P_i from the column axis. In this way, the NeReBot configuration can be optimized for a specific rehabilitation exercise. Machine and patient shoulder reference frames are also shown.

Fig. 3. NeReBot splint close-up. Patient's hand is supported by a hemispherical plastic component, while the forearm is fastened by three fabric strips. Front wire magnetic fasteners are also shown.

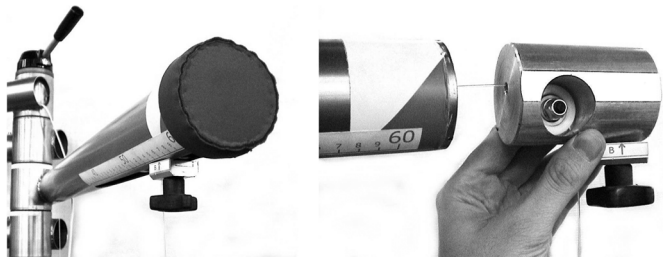

Fig. 4. Wire-entry-point regulation system. To the left is a close-up of the end of the arm. To the right is the aluminium cylinder which can be moved inside the hollow arm to change wire entry point position; the black knob is used to lock the cylinder.

significant gains in motor function after stroke which do not end at discharge from inpatient rehabilitation [22]), when firstly passive therapy and subsequently active assistive therapy can be delivered. A series of clinical trials have been conducted with this in mind. The aims of these trials were to: 1) compare motor-functional recovery of patients undergoing conventional therapy augmented with robotic therapy to a control group that received conventional therapy only; 2) evaluate adverse effects; 3) evaluate toleration and acceptance of the machine by patients.

This paper addresses not only the mechanical and control system design issues, but also presents clinical trials. The paper is divided as follows: Section II describes the mechanical structure of the NeReBot, Section III addresses working space optimization, Section IV illustrates control system design and implementation, and Sections V and VI present the treatment protocol and clinical results.

II. Mechanical Design

Fig. 2 shows a diagram of the mechanical structure of NeReBot. The base of the robot is designed in such a way that the patient can be treated while sitting in a wheelchair (Fig. 1) or lying in a hospital bed. The base consists of a C-shaped frame, featuring omnidirectional wheels that can fit under any commercial hospital bed. A square section column is fixed on the central part of the base, holding three horizontal round-section, hollow aluminium arms on top, which support the wires. One end of each wire is fastened to the patient's arm by means of a special splint (shown in Fig. 3). Let P_{fi} be the point of the splint to which the wire is attached (where subscript $i = 1, 2, 3$ indicates the wire). The other end of the wire enters the robot arm at point P_i, proceeds through the arm towards the central column and then runs down alongside the column. The wire is eventually wound around a pulley located at the base of the robot. Each pulley is directly driven by a MAE M 642–1340 dc electric motor, equipped with a BHK 16.05A1000-I2-5 1000ppr incremental encoder. Each motor is powered by an Advanced Motion Controls 25A8 PWM servo amplifier. The amplifiers and all power supply components fit in an isolated box located at the base of the robot.

Different kinds of wires have been tested. The optimum wire in terms of elasticity, strength, motion smoothness, and surface acceptability proved to be a 1-mm-diameter nylon wire. To improve safety, the wire is connected to the splint by means of a magnetic fastener (see Fig. 3), which disconnects whenever the tension applied to the wire exceeds a given value. By replacing the magnetic insert, different maximum tension values can be set, according to the patient's arm weight; 30 N and 50 N were employed during clinical trials. Moreover, the motor's maximum continuous torque and pulley radius have been chosen so that maximum wire tension does not exceed a value of 100 N.

To prevent the patient from feeling reducer-related friction, no gear reducer is employed. Accordingly, there is no need to measure wire tension during therapy, since its value can be reliably estimated as a linear function of the commanded torque (for static tests accuracy error is $\pm 5\%$). This neglects dynamic effects of the electric motor, but the assumption is supported by the fact that speed and acceleration are very low. One drawback to this choice is that high rotational speeds could be reached, since the motor is directly driven. To avoid this problem, we introduced some redundant speed control checks and a watchdog timer, which power off the system in the event of failure. Three alarm buttons complete the security system; one of them can be held by the operator or the patient him/herself, the second one is mounted onto the central arm, and the third one is fixed on the power box. The electrical motors are shut down by pressing

TABLE I
OPTIMAL CONFIGURATION OF THE NEREBOT CALCULATED USING THE SOFTWARE OPTIMIZATION TOOL FOR THE AVERAGE ITALIAN MALE (80 KG MASS, 1,75 M HEIGHT). PATIENT'S SHOULDER POSITION IS CALCULATED IN THE NEREBOT REFERENCE FRAME SHOWN IN FIG. 2. ARM EXTENSION EXERCISE IS A 3-D. TRAJECTORY OF THE ARM WHICH INVOLVES ABDUCTION, SHOULDER FLEXION, AND ELBOW FLEXION

Exercise	Arm#1		Arm#2		Arm#3		Patient's shoulder		
	$\vartheta_1[^\circ]$	$s_1[mm]$	$\vartheta_2[^\circ]$	$s_2[mm]$	$\vartheta_3[^\circ]$	$s_3[mm]$	$y[mm]$	$y[mm]$	$z[mm]$
Abduction (chair)	-65	450	32	370	-30	500	600	150	1010
Abduction (bed)	-74	500	48	450	-38	680	550	330	1300
Elbow flexion	-85	450	60	370	-15	470	420	130	1010
Arm extension	-66	450	24	550	0	650	650	500	1010
Pronosupination	-40	400	15	370	-15	610	500	100	1010

these buttons and an emergency procedure is spawned by the controller. As a consequence, the patient's arm falls down very smoothly with no risk at all for the patient.

The mechanical structure is fitted with frame-setting mechanisms in order to adapt the robot to the needs of the patient and therapy. A screw-jack mechanism is located inside the square column, so that the vertical position of the three arms can be changed. In addition, a knob located at the robot top (see Figs. 1 and 4) can be used to unlock the arms. By doing so, the therapist can set the angular position ϑ_i of each arm before beginning the therapy (in fact, the arms can be rotated around the column axis, see Fig. 2). Once the configuration has been chosen, the operator shuts the knob blocking all arm rotations simultaneously. Finally, the distance s_i of points P_i from the column axis can be set independently (the wire entry point setting mechanism is shown in Fig. 4). In this way, the NeReBot configuration can be optimized with respect to the arm (left or right), the size of the patient and the kind of exercise to be performed (please refer to Section III for more details).

III. WORKING SPACE OPTIMIZATION

Each exercise is recorded by manually moving the patient's forearm while the motors produce a constant torque to keep all wires stretched. When a certain position is reached, the therapist stores the motor angular positions in the control system by pressing a button (*learning phase*). The machine then interpolates acquired data to obtain cubic-spline joint trajectories, which produce very smooth spatial motion of the patient's arm (*therapy phase*). During therapy, the wire length is controlled by each motor, while the speed of the exercise can be changed by the therapist.

It has been demonstrated that to move a rigid body in 3-D space without any other external force acting on it, at least seven wires are required to produce three forces and three torques, since each wire-drum-motor system can only pull [23]–[25]. In the case of the NeReBot, the patient's arm connected to the three wires of NeReBot represents a different system: the kinematic chain of the patient's arm has 5 DoF (3 DoF for the shoulder, 1 DoF for elbow flexion–extension, and 1 DoF for forearm supination/pronation). The external forces acting on this system are the three wire tensions and the force of gravity of the arm itself, which can be considered the fourth, downward-oriented external force. By controlling the motor torques, the three wires can generate three generic forces on the splint. Although the resultant of these forces can never be downward oriented, the force of gravity of the patient's arm will help to generate forces in that direction.

With this configuration, not all 5 DoF can be controlled for the arm, since the wires provide only three unidirectional constraints. As a result, for a given (controlled) value of wire lengths l_i, the patient's forearm can still swing over an approximately horizontal surface. Since this results in the patient feeling guided rather than restrained by the machine, and very smooth, comfortable motion is achieved, this behavior can be considered acceptable and is highly appreciated by patients and therapists. The working space of NeReBot is, however, rather limited in the horizontal direction. On the other hand, the robot has a very simple mechanical structure and control system, and the mechanical structure can be manually adjusted before beginning therapy to adapt the working space to a specific exercise (see Table I for details).

To evaluate the effective capabilities of NeReBot, a software simulator was conceived and implemented to address static interaction between the NeReBot and the patient's arm (Fig. 5). This tool is designed to define the desired arm trajectory (in terms of arm joint rotations), to simulate its execution by NeReBot, and to compare the desired arm joint angles to the ones obtained during the robot-aided therapy.

Let vector $\mathbf{v} = \{\alpha_1, \alpha_2, \alpha_3, \alpha_4, \alpha_5\}$ define the configuration of the patient's arm, where angles $\alpha_1, \ldots, \alpha_5$ indicate shoulder, elbow and ulna-radius rotations (one spherical and two revolute joints). The arm model employed does not account for the translational degrees of freedom of the shoulder; this simplification was introduced since the patient's shoulder is usually supported by a fabric strip during therapy (see Fig. 2), while the trunk is fastened onto the chair. During the learning phase, the patient's arm is moved by the therapist to a set of n locations. Let $\mathbf{v}_j = \{\alpha_{1j}, \alpha_{2j}, \alpha_{3j}, \alpha_{4j}, \alpha_{5j}\}$ $(j = 1, \ldots, n)$ be the arm configuration in the jth location. The desired patient's arm trajectory $\mathbf{v}^{\mathrm{des}}(t)$ is obtained by cubic-spline interpolation of vectors $\mathbf{v}_j$.[1]

Let $\mathbf{q}_j = \{q_{1j}, q_{2j}, q_{3j}\}$ $(j = 1, \ldots, n)$ be the set of motor angular positions corresponding to the arm configuration $\mathbf{v}_j$. Vector $\mathbf{q}_j$ can be calculated as a function of vector

[1]This is an assumption of the software simulator, since the only information given by the therapist is a set of arm positions.

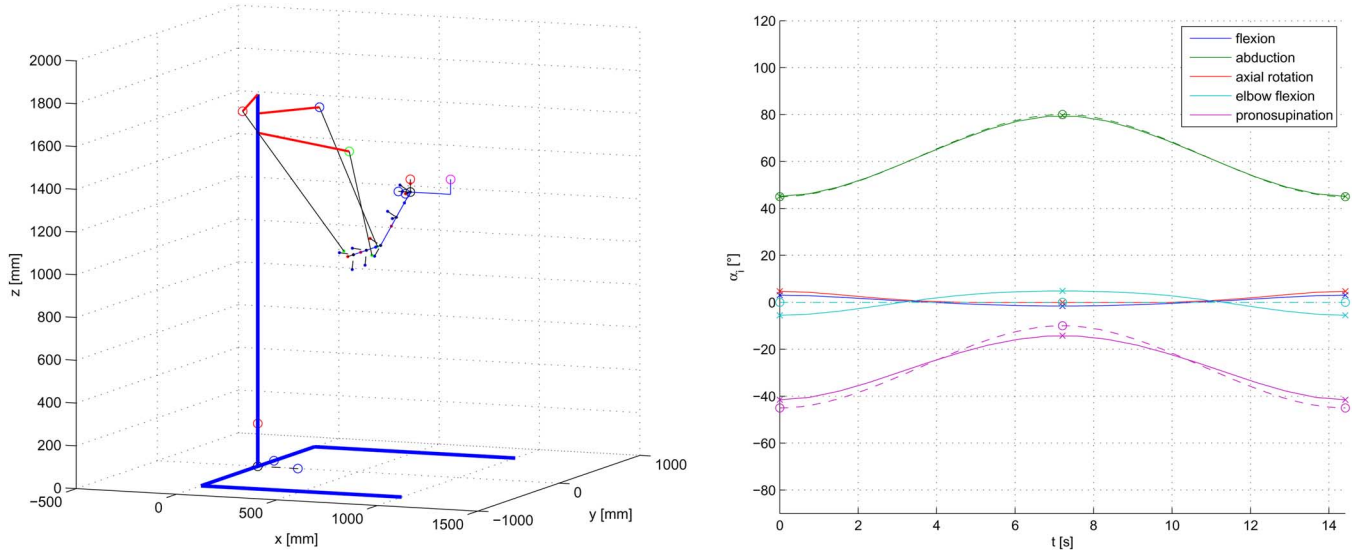

Fig. 5. Simulation of an abduction–adduction therapy. To the left is the diagram of the NeReBot structure and the patient's arm. To the right is the plot of joint angles versus time for the first cycle of simulated therapy. Continuous lines represent the resulting arm–joint values while the round spots are the via-points chosen by the therapist. Dotted lines represent a cubic spline interpolation of the via-points, which can be considered a reasonable target value for arm–joint angles. As we can see, the abduction–adduction angle of the shoulder (green line on top) follows a very accurate, smooth trajectory, while all other arm angles are kept within a suitable range (nearly $\pm 5^\circ$) from their target value.

$\mathbf{v}_j$, of the patient's shoulder position $\mathbf{x} = \{x, y, z\}$ in the NeReBot reference frame[2], of the NeReBot structure configuration $\mathbf{c} = \{\vartheta_1, \vartheta_2, \vartheta_3, s_1, s_2, s_3\}$, and of the wire tension used during the learning phase. The reference trajectory for NeReBot motors $\mathbf{q}^{\text{ref}}(t) = \left\{q_1^{\text{ref}}(t), q_2^{\text{ref}}(t), q_3^{\text{ref}}(t)\right\}$ is thus obtained by interpolating vectors $\mathbf{q}_j$, according to the trajectory planner implemented in the NeReBot controller, which takes into account some speed and acceleration constraints.

As far as the arm model is concerned, the patient's arm is made up of two rigid bodies, the forearm and the upper arm, whose mass and center of mass are m_f, m_u, G_f, and G_u, respectively.[3] Centers of mass are a function of shoulder position and arm joint angles

$$G_u = G_u(x, y, z, \alpha_1, \alpha_2, \alpha_3) = G_u(\mathbf{x}, \mathbf{v})$$
$$G_f = G_f(x, y, z, \alpha_1, \alpha_2, \alpha_3, \alpha_4, \alpha_5) = G_f(\mathbf{x}, \mathbf{v}).$$

At a given configuration of NeReBot $(\tilde{\mathbf{q}}, \tilde{\mathbf{c}})$ and patient's shoulder position $\tilde{\mathbf{x}}$, the potential energy of the patient's arm connected to the NeReBot is given by

$$\prod(\tilde{\mathbf{x}}, \mathbf{v}, \tilde{\mathbf{q}}, \tilde{\mathbf{c}}) = (m_f G_f + m_u G_u)\{0, 0, g\}^T + \frac{1}{2}\sum_{i=1}^{3} k_i \Delta l_i^2 \quad (1)$$

where g is the gravity acceleration, Δl_i is the ith wire stretching and k_i is the ith wire stiffness. If the therapy is performed in quasi-static conditions (very low speed and acceleration) and the patient does not exert any force on the splint (passive behavior), the configuration of the arm during therapy $\tilde{\mathbf{v}}$ will be the one and only factor to minimize the potential energy given by (1)

$$\tilde{\mathbf{v}} = f(\tilde{\mathbf{x}}, \tilde{\mathbf{q}}, \tilde{\mathbf{c}}) = \left\{\mathbf{v} \in \Re^5 : \frac{\partial \prod(\tilde{\mathbf{x}}, \mathbf{v}, \tilde{\mathbf{q}}, \tilde{\mathbf{c}})}{\partial \mathbf{v}} = 0\right\}.$$

The potential energy does not have local minima. During therapy, assuming that $\mathbf{q}(t) \cong \mathbf{q}^{\text{ref}}(t)$ (i.e., negligible motor position tracking errors), the actual trajectory of the arm $\mathbf{v}^{\text{act}}(t) = f(\tilde{\mathbf{x}}, \mathbf{q}^{\text{ref}}(t), \tilde{\mathbf{c}})$ can be estimated as

$$\mathbf{v}^{\text{act}}(t) = \left\{\mathbf{v} \in \Re^5 : \frac{\partial \prod(\tilde{\mathbf{x}}, \mathbf{v}, \mathbf{q}^{\text{ref}}(t), \tilde{\mathbf{c}})}{\partial \mathbf{v}} = 0\right\}.$$

In conclusion, for a given therapy $\mathbf{v}_j$ $(j = 1, \ldots, n)$, the software simulator can estimate the real motion of the arm $\mathbf{v}^{\text{act}}(t)$ and compare it with the desired one $\mathbf{v}^{\text{des}}(t)$. By changing NeReBot configuration vector $\tilde{\mathbf{c}}$ and shoulder position $\tilde{\mathbf{x}}$, the simulator can be used to find the optimal machine setup for a given therapy, i.e., the robot configuration and patient position which minimize the difference between the desired and the actual motion of the patient's arm, in terms of arm joint angles. This tool has been used extensively, resulting in a table containing the optimal machine setup data for the exercises most commonly required by medical staff. These trajectories have been tested for variously sized patients, using the Dempster table [26]. Results for the average Italian male (80 kg mass, 1,75 m height) are presented in Table I, which contains optimal robot configuration parameters and patient positioning data for the most common exercises (the patient's shoulder position is expressed in the machine base reference frame shown in Fig. 2). These results apply to patients of different sizes and weights within a reasonably wide range: the optimal configuration depends very much on the exercise to be executed and very slightly on patients' arm dimensions and masses.

[2]Since the splint is rigidly connected to the forearm, points P_{fi} are a function of arm angles and shoulder position.

[3]These data have been estimated using the Dempster table [26].

IV. Control System

During the initial trials a typical PD controller was employed to control each motor position q_i. Hence, the control action was $\tau_i = k_P e_i + k_D \dot{e}_i$, where τ_i is the torque exerted by the ith motor, k_P and k_D are proportional and derivative gains, and $e_i = q_i^{\text{ref}} - q_i$ is the error. In order to render interaction between robot and patient smooth and nontraumatic, the value of k_P was very low. This solution caused problems during passive movements (especially in the case of patients lying in bed), since high errors e_i occurred. To avoid this problem, strong integral action has been introduced into the control. However, it is well known that high integral gains can cause overshoot: a problem which can be solved with anti-wind-up techniques [27]. A new, rather than a state-of-the-art, anti-wind-up technique was proposed, which exploits the fact that wire-based robots are unilaterally actuated. A switching PID control has been used, whose control action is

$$\tau_i = \begin{cases} k_P e_i + k_D \dot{e}_i + k_{I+} \int e_i dt & \text{if } e_i < 0 \\ k_P e_i + k_D \dot{e}_i + k_{I-} \int e_i dt & \text{if } e_i \geq 0 \end{cases}$$

where $k_{I-} \gg k_{I+}$. This avoids high overshoot thanks to the small value of k_{I+}.

The NeReBot control software has been implemented in C standard language, and is made up of two separate modules: a high-level module for managing the user interface and a low-level module for multiaxis control. The former is a non-real-time software package operating in the Windows 2000 environment. Basically, it takes care of the graphics and handles interaction with the user. The GTK+ open source multiplatform library has been employed for the graphics. Patient data and treatment session data are saved in an embedded database, based on the Berkeley DB. The second module, which is real-time, is responsible for low level control of each axis. It implements a modified switching PID position controller and several safety checks in order to predict failures which could hurt the patient and/or therapist. The real-time module has been implemented exploiting the developing library software distributed by VCI (VenturCom) written for Windows 2000 kernel, which represents a cheap but fully reliable choice. The two modules (real time and non real time) share data by means of IPC (Inter Process Comunication) mechanisms. In particular, semaphores and share memory tools have been employed. A Quanser Multi-Q PCI data acquisition board has been used for I/O. The board acquires three differential encoder input signals and three differential analog input signals (proportional to each motor torque), and provides the three differential analog reference signals for the motor amplifiers. A sample-rate of 2 KHz has been chosen. Graphics are updated at a frequency of 50 Hz without any appreciable slowing down in speed. The software has been tested on an Intel Pentium 4 PC (1.7 MHz and 256 Mb RAM memory).

PID parameters were tuned during laboratory tests in such a way as to avoid vibrations (instability) and at the same time obtain small position errors. The maximum overall position error measured during lab and clinical trials is less than 5 mm, in terms of length error for a single wire. This value is fully satisfactory for our application. It is emphasized that the error remains close to the maximum value of 5 mm just for a short time, namely until the control integral action drastically reduces its value. Anyway, since all the wires originate from the upward direction and are all connected to the splint, the splint position error fits the same range of the single wire error.

V. Motor Task and Treatment Protocol

A. Population

Twenty-four hemiparetic/hemiplegic patients (13 males and 11 females), mean age 67.5 years (range 48–79 years), consecutively admitted to the Rehabilitation Unit of Padova University Hospital after first, single, unilateral, ischemic stroke were enrolled for the clinical trials. The diagnosis of stroke was based on clinical assessment (presence of motor and possibly sensory deficits) and confirmed by instrumental assessment (computerized axial tomography [CT] or nuclear magnetic resonance [NMR]), in accordance with World Health Organization criteria [28]. The following exclusion criteria were adopted for the study: 1) previous stroke or transitory ischemic attacks; 2) bilateral stroke lesion or diffuse cerebral vasculopathy; 3) severe neuropsychological impairment (global aphasia or severe attention deficit) affecting participation in rehabilitation; 4) presence or appearance of complications (cardiovascular, infectious, deep vein thrombosis, etc.) during hospital stay that might prevent the patient from undergoing rehabilitation treatment; 5) patients older than 80 years. This study was approved by the Ethical Committee of Padova University Hospital, and informed consent was obtained from all patients.

All patients consecutively admitted to the study were randomized to an Experimental Group (EG, 12 patients) or Control Group (CG, 12 patients). The patients of both groups admitted to the trial received the same dose and length per day of standard rehabilitative treatment (based on the Bobath concept, including transfer, and gait training) and occupational post-stroke therapy (emphasizing ADL performance) from the same blinded interdisciplinary clinical team according to a rehabilitation project. The 12 patients in the EG received additional early robotic training by NeReBot, including at least 40 sessions (two sessions per day, lasting about 20–25 min each, five days a week, for four weeks). The CG was exposed to the robotic device 30 min, twice a week, but the exercises were performed with the unimpaired upper limb. Treatment was completed in the same rehabilitation center for all the recruited subjects during hospitalization and no patient underwent rehabilitative treatment elsewhere during follow-up until the final assessment.

B. Evaluation Procedure

At the start and at the end of the trial (three months after stroke, i.e., seven weeks after the end of robot therapy), a standard assessment procedure was used to evaluate all patients (EG and CG). Assessments were performed for all patients involved in the study by the same blinded clinician (SM) who had previously been trained to use the scales. Physiotherapy and nursing staff had also been trained in the months prior to the survey. The clinician was not directly involved with the rehabilitative therapy (robot-assisted therapy or standard therapy) and did not know who was enrolled in the EG or CG. The standard assessment procedure included: the Medical Research Council (MRC)

score, the upper limb subsection of the Fugl-Meyer (FM) score and the Motor Status Score (MSS), the Functional Independence Measure (FIM), and its motor component (motFIM).

The MRC is an ordinal scale for measuring muscle strength of muscle force (range: 0–5 for each joint; where $0 = \text{no muscle contraction}$; $5 = \text{normal strength}$) in isolated or muscle groups. This scale was used to rate the strength of the paretic arm during six actions: shoulder flexion and abduction (MRC shoulder), elbow flexion and extension (MRC elbow), and wrist flexion and extension (MRC wrist) [29].

The FM is a scale that measures motor impairment [30], [31]. The validity and repeatability of this scale have been established [32]. The test includes items related to movements of the shoulder, elbow, forearm (proximal arm), wrist and hand (distal arm). The total score ranges from 0 to 66. We considered the shoulder/elbow and coordination subsections (FM-SEC; 42 out of 66 items) and the wrist/hand subsection (WH, 24 out of 66 items). We examined proximal and distal components of the FM separately to enable measurement of each trained limb segment.

The Motor Status score (MSS) provided a more complete, discrete measure of upper-limb isolated movements and motor function than the FM test, by grading motor abilities on a well-defined six-point scale [33], [34]. Motor function is defined as the ability to accomplish movements or tasks that are essential components of activities of daily living [35]. The MS score was divided into two scales: the first for shoulder and elbow movements that were exercised by the robot (MS-SE; maximum score 40) and the second for wrist and finger movements that were not exercised by the robot (maximum score $= 42$).

The FIM is an ordinal scale that assesses severity of motor and neuropsychological disability and amount of treatment needed for each patient admitted to a rehabilitation facility [36], [37]. The FIM is composed of 18 items divided into seven levels (minimum score: 18, maximum score: 126, equivalent to total functional independence). The motor component (motFIM) is represented by 13 items on seven levels, (minimum score: 13, maximum score: 91). They include self-care, sphincter control, mobility, and locomotion.

In addition, subjects were asked to report the amount of pain they experienced in the affected shoulder by the visual-analogue scale (VAS), consisting of a 100-mm line ($0 = \text{no pain}$; 100 high pain); other complications, such as the development of shoulder–hand syndrome, were also recorded. Lastly, at the end of robot training, we measured the degree of acceptance of robot therapy by the visual-analogue scale (VAS), consisting of a 100-mm line ($0 = \text{poor tolerance}$; 100 high tolerance).

C. Intervention

Training by NeReBot consisted of peripheral manipulation of the shoulder and elbow of the impaired limb correlated with visual stimuli (visual feedback). The NeReBot training was supervised by the same therapist for all patients but a different therapist performed standard rehabilitation. Each therapy session began with clinical examination of the impaired upper limb, to investigate motor function recovery, pain, or other complications. At the start of each session, the trained researcher (therapist) sought to identify the optimal path and rest positions for each patient within the robot working space, based on individual stage of recovery, in order to fully exploit the patient's residual motor skills. The assigned tasks were limited to impaired shoulder and elbow motor performance since the wrist and hand were restrained by the orthesis. Patients performed five to seven exercise cycles lasting 3 min each, followed by a 1 min resting period (total time for each session: approximately 20–30 min). The exercise protocols focused on shoulder and elbow movement patterns and included alternative flexion/extension (elbow), adduction/abduction (shoulder), and prono-supination (forearm) movements (about 20 repetitions per cycle).

A trained research assistant provided a standardized set of instructions and was always in attendance to indicate positions and useful trajectories of movement for the upper limb and, if necessary, to intervene in emergency situations. The robot assisted and guided the patient's forearm and hand through a repetitive pattern set by the rehabilitation team, based on degree of patient impairment.

After the therapist had chosen the exercise, motors were activated in order to prevent wire slack. Then the therapist manually led the patient's arm along a number of via-points. These points were recorded and employed by the path planner module to plan the whole trajectory. Eventually, the robot autonomously moved the patient's arm according to the calculated trajectory. Motion speed was set by the operator in the range of 5–60 mm/s. Patients were instructed to remain passive as the robot moved their limb along the programmed trajectory for the first time. After that, they were asked to actively contribute to the motion. During the therapy session, both the clinician and video feedback encouraged patients to increase their effort. Visual feedback consisted of a 3-D image of a virtual upper limb, with three arrows intuitively showing the patient the forces currently applied to the limb by the wires (and hence the desired direction of motion). This helped guide the patient through correct execution of the exercise. A repetitive sound signal was also provided, but not related to the patient's effort; sound level was increased to indicate the start and the end of the exercise. This acoustic and visual feedback was a very useful means of maintaining a high level of patient attention throughout the session.

During the first week of treatment the patient was usually supine (in bed) and daily exercises consisted mainly of passive repetitions along simple trajectories, e.g., arm elevation. After the first week, the set of exercises was extended and became more complex, with employment of circular, spatial, and multi-DoF active-assistive movements. The patient sat on a chair or wheelchair fitted with seat-belts to limit torso movements and to avoid falls. The therapy addressed the impaired shoulder and elbow, while the wrist and hand were immobilized by the orthesis (only pronation-supination of the forearm was left free). Motion speed was also increased according to patient improvements. Movements were performed slowly to avoid abnormal muscle activity that could cause pain or abnormal activity by hyperreflexia of the paretic muscle.

D. Statistical Analysis

The baseline characteristics of the patients in the control and experimental groups were compared by Chi square tests (nominal data) or Mann-Whitney U tests (ordinal data). We adopted a

TABLE II
PATIENTS' DEMOGRAPHIC AND CLINICAL CHARACTERISTICS MEASURED AT REHABILITATION ADMISSION (MEAN AND STANDARD DEVIATION)

Characteristics	EG ($n = 12$)	CG ($n = 12$)	p
Sex M/F	7/5	6/6	Ns
Disabled limb (L/R)	5/7	4/8	Ns
Age (y)	63.4 ± 11.8	67.8 ± 9.9	Ns
Time post-stroke (dy)	5.1 ± 2.1	5.5 ± 3.2	Ns
Total days in rehabilitation (dy)	46.4 ± 25.5	47 ± 28.0	Ns
MRC shoulder (range 0-5)	1.8 ± 2.5	1.5 ± 1.8	Ns
MRC elbow (range 0-5)	1.9 ± 1.8	1.5 ± 1.9	Ns
MRC wrist (range 0-5)	0.7 ± 1.0	1.0 ± 1.3	Ns
FM-SEC (range 0-42)	10.1 ± 8.7	11.8 ± 10.2	Ns
FM-WH (range 0-24)	1.5 ± 2.3	1.8 ± 3.1	Ns
MSS-SE (range 0-40)	4.3 ± 3.1	3.8 ± 3.4	Ns
MSS-WH (range 0-42)	0.5 ± 0.4	0.7 ± 0.5	Ns
MotFIM (range 13-91)	32.9 ± 12.7	24.1 ± 13.1	0.050
FIM (range 18-126)	65.1 ± 14.7	55.6 ± 17.1	Ns

single baseline (the shortest possible baseline for this kind of patients) since our goal was to investigate the effects of very early training. We performed Mann-Whitney U tests to identify any significant differences between average gains in score on motor or functional impairment (FM, MSS, FIM, motFIM) in the two groups at the final evaluation. Statistical significance was set at $p < 0.050$. The statistics were processed using SPSS version 11.5 (SPSS Inc., Chicago, IL).

VI. CLINICAL RESULTS

The CG and the EG were matched for age, gender, time between onset of the stroke and admission to the rehabilitation center and total days in standard rehabilitation. Moreover, the two groups were comparable in terms of initial impairment and disability (initial clinical measures are summarized in Table II). NeReBot training started on average 7.5 days after stroke (range 5–9 days). Furthermore, the number of patients in each group with medical comorbidity (hypertension, coronary artery disease, diabetes mellitus, infection, or depression) was comparable (χ^2 range: 0.1–0.7).

The results of the assessment at three months after stroke are summarized in Table III. The MRC motor power test for shoulder ($p = 0.045$) and elbow ($p = 0.050$), FM-SEC test ($p = 0.010$), MSS-SE ($p = 0.010$), motFIM ($p = 0.004$), and FIM ($p = 0.035$) showed significant effects of robot therapy. Since the two groups received a different total amount of intervention, this result is likely to be related to the increased amount of treatment received by the EG group. For this reason, further clinical trials are currently being planned, with the aim of comparing robot therapy to conventional therapy. The other evaluation scales (wrist/hand subscale) showed a slightly positive but nonsignificant trend.

No differences were found between the two groups in terms of joint-related pain in the shoulder, wrist, or hand, or any other complications, including shoulder–hand syndrome. Two patients from the EG and one from the CG developed shoulder–joint pain which did not influence performance of the rehabilitation program; one patient from the CG developed shoulder–hand syndrome. No adverse effects occurred during robot-assisted therapy in the EG.

TABLE III
AVERAGE GAINS (MEAN ± SD) IN THE FUGL-MEYER SCORE FOR SHOULDER, ELBOW ,AND COORDINATION (FM-SEC) AND FOR WRIST AND HAND (FM-WH), MOTOR STATUS SCORE FOR SHOULDER AND ELBOW (MS- SE) AND WRIST AND HAND (MS-WH), MOTFIM AND FIM AT THE FINAL ASSESSMENTS (THREE MONTHS AFTER STROKE) IN THE EG AND CG

Scale	EG ($n = 12$)	CG ($n = 12$)	p
MRC shoulder (range 0-5)	2.5 ± 1.2	0.9 ± 1.0	0.045
MRC elbow (range (0-5)	1.7 ± 1.2	1.1 ± 0.9	0.050
MRC wrist (range 0-5)	1.7 ± 1.8	2.2 ± 1.2	0.215
FM - SEC (range 0-42)	17.2 ± 6.5	8.9 ± 8.3	0.010
FM- WH (range 0-24)	5.5 ± 3.3	3.7 ± 2.5	0.210
MSS-SE (range 0-40)	12.5 ± 4.0	8.5 ± 5.4	0.010
MSS-WH (range 0-42)	0.8 ± 0.2	0.6 ± 0.4	0.390
MotFIM (range 13-91)	33.2 ± 7.5	16.5 ± 10.2	0.004
FIM (range 18-126)	40.1 ± 8.2	26.1 ± 10.1	0.035

The questionnaire administered to the EG patients (by VAS) showed that the robotic intervention was well accepted (mean score 85.3/100). All of them strongly recommended including the robot therapy in the rehabilitation program.

VII. CONCLUSION AND FUTURE RESEARCH

We presented the design of a wire-based robot for neurorehabilitation, called the NeReBot. Although the robot has only 3 DoF, it is capable of moving the patient's arm along nontrivial spatial paths according to the required therapy, which can be set by the rehabilitation therapist thanks to a very simple teaching-by-showing procedure. Our main challenge was to deliver the therapy from a very early stage, i.e., right after the stroke event. To the best of our knowledge, NeReBot is the first robot capable of delivering early robot-aided poststroke therapy. The study revealed statistically significant benefits of the additional robotic therapy in persons with a paralyzed or paretic upper limb after stroke. In these patients, an early robotic approach may usefully complement other treatments by reducing motor impairment during both the acute and chronic phases of stroke recovery.

The robot-guided training involved repetitive passive and active-assistive exercises of the shoulder and the elbow. Robot-aided training focused on the shoulder and elbow while the wrist and hand were splinted. As a result, the robot group presented significantly greater improvements in their proximal arm FM scores compared to the control group, but the change in distal arm FM scores did not differ significantly between the two groups.

Although the robot therapy lasted only four weeks, patients of the EG showed motor and functional improvements compared to the control group even three months after the stroke event. We believe that this result reflects the persistent effect potentially delivered by the additional robot therapy. Further clinical trials will be needed to assess the effectiveness of robot therapy with respect to conventional therapy.

One limitation of the study is that the outcome measures were not evaluated immediately after the conclusion of robotic

therapy. Therefore, it is impossible to know what portion of the group differences were directly related to the robotic therapy. For example, patients in the robotic therapy group may have developed the habit of moving their limb more than the control group, and continued greater use after therapy, thereby amplifying the training effect. This point will be more deeply investigated in further clinical trials.

The use of FIM score can be a weakness point in the design and in the evaluation of our results, because gains in motor function have not always been reported to translate into significant improvement in the performance of basic self-care activities. In fact, the relationship between upper extremity Fugl-Meyer and the self-care component of the FIM is modest at best, because the FIM self-care component measures general disability and is not arm-disability specific [38]. So the significant improvement presented by most of our patients after robot training is particularly interesting, but others tools of measure are desirable.

During the initial lab and clinical trials, some limitations of the NeReBot did arise. First, moving the robot through the hospital ward can sometimes be difficult, due to the dimensions and weight of the robot base. Second, the working space does not always meet therapists' requirements (some horizontal movements of the upper limb cannot be performed properly). Third, manual setup of the machine structure prior to treatment proved to be a rather awkward procedure, and the final result is operator-dependent. Finally, the hardware/software configuration of the control system can be further improved. Nevertheless, since the wire-drive philosophy has produced many benefits, a new robot based on the same concept has been designed and is currently undergoing lab tests.

REFERENCES

[1] G. B. Prange, M. J. Jannink, C. G. Groothuis-Oudshoorn, H. J. Hermens, and M. J. IJzerman, "Systematic review of the effect of robot-aided therapy on recovery of the hemiparetic arm after stroke," *J. Rehabil. Res. Develop.*, vol. 43, pp. 171–184, 2006.

[2] P. S. Lum, C. G. Burgar, P. C. Shor, M. Majmundar, and H. F. Van der Loos, "Robot-assisted movement training compared with conventional therapy techniques for the rehabilitation of upper limb motor function following stroke," *Arch. Phys. Med. Rehab.* , vol. 83, no. 7, pp. 952–959, 2002.

[3] B. T. Volpe, H. I. Krebs, N. Hogan, I. Edelstein, C. Diels, and M. L. Aisen, "A novel approach to stroke rehabilitation: Robot-Aided sensorimotor stimulation," *Neurology*, vol. 54, pp. 1938–1944, 2000.

[4] S. Barreca, S. L. Wolf, S. Fasoli, and R. Bohannon, "Treatment interventions for the paretic upper limb of stroke survivors: A critical review," *Neurorehabil. Neural Repair*, vol. 17, pp. 220–226, 2003.

[5] G. Kwakkel, R. C. Wagenaar, J. W. Twisk, G. J. Lankhorst, and J. C. Koetsier, "Intensity of leg and arm training after primary middle-cerebral-artery stroke: A randomized trial," *Lancet*, vol. 354, no. 9174, pp. 191–196, 1999.

[6] H. M. Feys, W. J. De Weerdt, B. E. Selz, G. A. C. Steck, R. Spichiger, L. E. Vereeck, K. D. Putman, and G. A. Van Hoydonck, "Effect of a therapeutic intervention for the hemiplegic upper limb in the acute phase after stroke: A single-blind, randomized, controlled multicenter trial," *Stroke*, vol. 29, pp. 785–792, 1998.

[7] J. Liepert, H. Bauder, H. R. Wolfgang, W. H. Miltner, E. Taub, and C. Weiller, "Treatment-induced cortical reorganization after stroke in humans," *Stroke*, vol. 31, pp. 1210–1216, 1999.

[8] C. Butefisch, H. Hummelsheim, P. Danzler, and K. H. Mauritz, "Repetitive training of isolated movements improves the outcome of motor rehabilitation of centrally paretic hand," *J. Neurological Sci.*, vol. 130, no. 1, pp. 59–68, 1995.

[9] H. I. Krebs, N. Hogan, M. L. Aisen, and B. T. Volpe, "Robot-aided neurorehabilitation," *IEEE Trans. Rehabil. Eng.*, vol. 6, no. 1, pp. 75–87, Mar. 1998.

[10] D. J. Reinkensmeyer, L. E. Kahn, M. Averbuch, A. N. McKenna-Cole, B. D. Schmit, and W. Z. Rymer, "Understanding and treating arm movement impairment after chronic brain injury: Progress with the arm guide," *J. Rehabil. Res. Develop.*, vol. 37, no. 6, pp. 653–662.

[11] P. S. Lum, C. G. Burgar, and P. C. Shor, "Evidence for improved muscle activation patterns after retraining of reaching movements with the MIME robotic system in subjects with post-stroke hemiparesis," *IEEE Trans. Neural Syst. Rehabil. Eng.*, vol. 12, no. 2, pp. 186–194, Jun. 2004.

[12] T. Nef and R. Riener, "ARMin: Design of a novel arm rehabilitation robot," in *Proc. IEEE 9th Int. Conf. Rehabilitation Robotics ICORR2005*, Chicago, IL, Jun. 2005, pp. 57–60.

[13] A. Toth, G. Fazekas, G. Arz, M. Jurak, and M. Horvath, "Passive robotic movement therapy of the spastic hemiparetic arm with REHAROB: Report of the first clinical test and the follow-up system improvement," in *Proc. IEEE 9th Int. Conf. Rehabil. Robot. ICORR2005*, Chicago, IL, Jun. 2005, pp. 127–130.

[14] N. Tejima, "Evaluation of rehabilitation robots for eating," in *Proc. 5th IEEE Int. Workshop Robot Human Commun. RO-MAN'96 TSUKUBA*, Tsukuba, Japan, Nov. 1996, pp. 118–120.

[15] Q. Meng and M. H. Lee, "Design issues for assistive robotics for the elderly," *Adv. Eng. Informatics*, vol. 20, pp. 171–186, 2006.

[16] Y. Takahashi and T. Kobayashi, "Upper limb motion assist robot," presented at the IEEE 6th Int. Conf. Rehabil. Robotics ICORR1999, Stanford, CA, Jul. 1999.

[17] S. Kim, M. Ishii, Y. Koike, and M. Sato, "Development of a SPIDAR-G and possibility of its application to virtual reality," in *Proc. ACM Symp. Virtual Reality Software Technol. VRST2000*, Seoul, Korea, Oct. 2000.

[18] R. C. V. Loureiro, C. F. Collin, and W. S. Harwin, "Robot aided therapy: Challenges ahead for upper limb stroke rehabilitation," presented at the IEEE Conf. Disability, Virtual Reality and Associated Technol., Oxford, U.K., Sep. 2005.

[19] D. Surdilovic, R. Bernhardt, and T. Schmidt, "STRING-MAN: A new wire robotic system for gait rehabilitation," presented at the IEEE 8th Int. Conf. Rehabil. Robotics ICORR2003, Daejeon, Republic of Korea, Apr. 2003.

[20] C. Fanin, P. Gallina, A. Rossi, U. Zanatta, and S. Masiero, "NeReBot: A wire-based robot for neurorehabilitation," presented at the IEEE 8th Int. Conf. Rehabil. Robotics ICORR2003, Daejeon, Republic of Korea, Apr. 2003.

[21] G. Rosati, P. Gallina, S. Masiero, and A. Rossi, "Design of a new 5 d.o.f. wire-based robot for rehabilitation," in *Proc. IEEE 9th Int. Conf. Rehabil. Robotics*, Chicago, IL, Jun. 2005, pp. 430–433.

[22] H. T. Hendricks, J. Van Limbeek, A. C. Geurts, and M. J. Zwarts, "Motor recovery after stroke: A systematic review of the literature," *Arch. Phys. Medicine Rehabil.*, vol. 83, pp. 1629–1637, 2002.

[23] Y. Shen, H. Osumi, and T. Arai, "Set of manipulating forces in wire driven systems," in *Proc. IEEE/RSJ/GI Int. Conf. Intell. Robots Syst.*, Sep. 1994, vol. 3, pp. 1626–1631.

[24] P. Gallina and G. Rosati, "Manipulability of a planar wire driven haptic device," *Mech. Mach. Theory*, vol. 37, no. 2, pp. 215–228, Feb. 2002.

[25] P. Gallina, G. Rosati, and A. Rossi, "3-d.o.f. wire driven planar haptic interface," *J. Intell. Robotic Syst.*, vol. 32, no. 1, pp. 23–36, 2001.

[26] D. A. Winter, Biomechanics and Motor Control of Human Movement.. New York, Wiley, 1990.

[27] A. H. Glattfelder, "Start-up performance of different proportional-integral anti-wind-up regulators," *Int. J. Control*, vol. 44, no. 2, pp. 493–505, 1986.

[28] "Stroke 1989: Recommendations on stroke prevention, diagnosis, and therapy," *Stroke*, vol. 20, pp. 1407–1431, 1989.

[29] Aids to the examination of the peripheral nervous system Medical Research Council, Her Majesty's Stationary Office, London, U.K., 1976.

[30] A. R. Fugl-Meyer and L. Jaasko *et al.*, "Post stroke hemiplegic patient," *Scand. J. Rehab. Med.*, vol. 7, no. 1, pp. 13–31, 1975.

[31] J. Sanford, J. Moreland, L. R. Swanson, P. W. Stratford, and C. Gowland, "Reliability of the fugl-meyer assessment for testing motor performance in patients following stroke," *Physical Therapy*, vol. 73, pp. 447–455, 1993.

[32] P. W. Duncan, M. Propst, and S. G. Nelson, "Reliability of the fugl-meyer assessment of sensorimotor recovery following cerebrovascular accident," *Physical Therapy*, vol. 63, pp. 1606–1610, 1983.

[33] M. L. Aisen, H. I. Krebs, N. Hogan, F. McDowell, and B. T. Volpe, Arch. Neurol. "The effect of robot-assisted therapy and rehabilitative training on motor recovery following stroke," 1997, vol. 54, pp. 443–446.

[34] S. E. Fasoli, H. I. Krebs, J. Stein, W. R. Frontera, and N. Hogan, "Effects of robotic therapy on motor impairment and recovery in chronic stroke," *Arch. Phys. Med. Rehabil.*, vol. 84, no. 4, pp. 477–482, 2003.
[35] P. S. Lum, C. G. Burgar, D. E. Kenney, and H. F. Van der Loos, "Quantification of force abnormalities during passive and active-assisted upper-limb reaching movements in post-stroke hemiparesis," *IEEE Trans. Biomed. Eng.*, vol. 46, no. 6, pp. 652–662, Jun. 1999.
[36] L. Tesio, C. V. Granger, L. Perucca, F. P. Franchignoni, M. A. Battaglia, and C. F. Russell, "The FIM instrument in the united states and italy: A comparative study," *Amer. J. Phys. Med. Rehabil.*, vol. 81, pp. 168–176, 2002.
[37] "Functional independence measure: Versione italiana—manuale d'uso," *Ricerca Riabilitazione*, vol. 2, pp. 1–44, 1992.
[38] J. C. Chae, M. V. Johnston, H. Kim, and R. D. Zorowitz, "Admission motor impairment as a predictor of physical disability after stroke rehabilitation," *Amer. J. Phys. Med. Rehabil.*, vol. 74, pp. 218–223, 1995.

Giulio Rosati received the M.Sc. degree in mechanical engineering from the University of Padua, Padua, Italy, in 1999, and the Ph.D. degree in applied mechanics at University of Brescia, Brescia, Italy, in 2003.

He has been Associate Professor of Applied Mechanics at the Faculty of Engineering, Department of Innovation in Mechanics and Management, University of Padua, Padua, Italy, since December 2006. He teaches mechanical systems control. He was Assistant Professor of Applied Mechanics at the same Faculty since January 2004. He was Visiting Professor at the Department of Mechanical and Aerospace Engineering of University of California, Irvine, in July 2007, within a research collaboration in the field of rehabilitation robotics. He was invited by Prof. D. Reinkensmeyer. His research interests include rehabilitation robotics, robotics (mainly, cable-driven systems), haptic interfaces, and industrial automation.

Paolo Gallina received the Ph.D. degree in applied mechanics from University of Brescia, Brescia, Italy, in 1999.

He was with the Faculty of Engineering of University of Padua, Padua, Italy, from 1999 to 2002, as Assistant Professor. He is currently Associate Professor of Applied Mechanics and Vibrations at the Department of Energetics, University of Trieste, Trieste, Italy. He was Visiting Professor at the Ohio University in 2000–2001. His interests are in vibrations, human–machine interfaces, and robotics, especially applied to rehabilitation.

Stefano Masiero graduated in Medicine and Surgery in 1990 and specialized in Physical Medicine and Rehabilitation in 1994 at Padua University, Padua, Italy.

He is an Assistant Professor at the Department of Medical and Surgical Sciences, Faculty of Medicine of Padua University and Surgeon's Assistant at the Department of Rehabilitation Medicine (Rehabilitation Unit) at Padua University Hospital, Padua, Italy. He currently lectures in physical medicine and rehabilitation at the undergraduate degree courses in medicine and surgery and physiotherapy at the University of Padua, Padua, Italy. His research interests are mainly focused on the application of robotic tools in the Neurorehabilitation setting.

Prof. Masiero is a member of the Italian Society of Physical and Rehabilitation Medicine and the Italian Society of Rehabilitation and Neurology.